Defence Science Journal, Vol 49, No 5, October 1999, pp. 393-409

Mixture Theory of Mass Transfer Based upon Microstructure

Robert L. Brown and Michael Q. Edens
Montana State Universes-Bozeman, Bozeman, MT-59 717-3900.

and

Michael Barber
Montana State University-Havre, Havre, MT-59 620.

ABSTRACT

A mixture theory has been developed to model equitemperature metamorphism of snow. This formulation is a volume fraction theory which models the interchange of mass between the constituents making up the mixture. The formulation has been developed so that the microstructure of the material is included to correctly describe the mechanical and thermal processes. The second law of thermodynamics is used to impose restrictions upon the various constitutive relations. These constitutive relations are then described in terms of microstructure of the material. The microstructure of each constituent is represented by constituent size (mean grain size, intergranular bond size), intergranular neck geometry, specific free surface area and dispersed density. The resulting formulation is then used to model equitemperature metamorphism of snow by determining the time-dependent changes in the distribution of grain size, neck size and dispersed densities of each of the constituents. The results obtained show that the formulation can describe how the material changes under equitemperature conditions. However, it is noted that since microstructure significantly affects the rate of metamorphism, an accurate determination of the microstructure (including grain and neck size distribution) is necessary for this approach to accurately predict changes in the material due to metamorphism.

NOMENCLATURE

v_α	Velocity vector
r_α	Partial density or dispersed density
ϕ_α	Volume fraction
θ_α	Absolute temperature
q_α	Heat flux
$\tilde{T}_\alpha$	Piola stress
T_α	Couchy stress tensor
b_α	Boly force
E_α	Lagrangian strain tensor
D_α	Rate of deformation tensor
L_α	Velocity gradient
F_α	Deformation gradient
u_α	Diffusion velocity
e_α	Thermal energy
ψ_α	Holmholtz free energy
η_α	Entropy
ma	Chemical potential
ξ_α	Internal state vector (to describe internal inelastic deformation processes)

Revised 23 August 1999

c_α Mass interaction

$\hat{P}_\alpha$ Momentum interaction

$\hat{e}_\alpha$ Energy interaction

1. INTRODUCTION

Since the early work of such pioneers as Truesdell[1] and Muller[2], mixture theories have slowly become recognised as a practical method for analysing complex materials composed of interacting constituents. Bowen[3] provided a comprehensive review of the advances in mixture theory up to that time. Since then, mixture theories have taken different forms and refinements[5-14].

The work presented here is a mixture theory based on the work of Hansen[12], *et al.* and Reid and Jafari[13], but is one that utilises the material microstructure to determine the manner in which the constituents interact, both chemically and mechanically. The examples provided here are restricted to the problem of equitemperature metamorphism, although the formulation can be applied to more general problems also. Equitemperature metamorphism represents a situation in which no external loads or temperature gradients are applied to the material. Under such conditions, the ice grains and the necks connecting the grains interchange mass. The necks acquire mass from all ice grains, and the small ice grains lose mass to the larger ice grains. The interchange of mass is facilitated by some ice surfaces losing mass to the pore vapour, while other surfaces simultaneously gain mass by deposition from the vapour. This process is driven by the surface energy and free surface area differences between various ice constituents.

This study is aimed to determine the specific details of this process. A properly constructed mixture theory can provide a clear picture of just how this complex array of grains and bonds interchange mass and how the internal material structure evolves. It will also provide a basis for further studies of the more complex problems of TG metamorphism.

Equitemperature metamorphism is an important process which affects the properties and longevity of snow roads and landing strips in polar regions. It also has applicability to snowmobile trails in alpine regions and vehicle mobility on natural snowcover. In addition, equitemperature metamorphism plays an important role in determining how an antarctic firn slowly consolidates into ice to form polar ice caps. It also has relevance to studies on how the ice caps will respond to global climate change. Finally, this process is relevant to thermal sintering of powdered metal compacts at elevated temperatures.

2. DEVELOPMENT OF MIXTURE THEORY

It is assumed that the mixture consists of N constituents. The index α will denote the α^{th} constituent, $a = 1,...,N$. Later, as one makes a specific application to a particular material, in the case of snow, the notation will become more specific. Since a volume fraction formulation is being used, the velocity of the mixture, v, is given by the following relation:

$$v = \sum_{\alpha=1}^{N} \phi_\alpha v_\alpha \tag{1}$$

The volume fractions ϕ_α for all the constituents must sum to unity

$$\sum_{\alpha=1}^{N} \phi_\alpha = 1 \tag{2}$$

For each constituent, the principles of balance of mass, linear momentum and energy are:

$$\frac{\partial \rho_\alpha}{\partial t} + div(\rho_\alpha v_\alpha) = \hat{c}_\alpha \tag{3}$$

$$\rho_\alpha v Y'_\alpha - div\,(\rho_\alpha v_\alpha) - \rho_\alpha b_\alpha = \hat{P}_\alpha \tag{4}$$

$$\rho_\alpha e Y'_\alpha - tr(T_\alpha D_\alpha) + div(q_\alpha) - \rho_\alpha r_\alpha + \hat{e}_\alpha = 0 \tag{5}$$

The principle of balance of angular momentum has not been discussed, since it is assume that the material does not possess measurable couple stresses. The mass interaction $(\hat{c}_\alpha)$, momentum interaction $(\hat{p}_\alpha)$, and energy interaction $(\hat{e}_\alpha)$ represent the rates per unit volume at which the α^{th} constituent is exchanging mass, linear momentum and energy, respectively with the other $(N\text{-}1)$ constituents.

The second law is assumed to have the following form for the mixture:

$$\sum_{\alpha=1}^{N}\left\{\begin{matrix}-\rho_\alpha\left(\eta_\alpha\theta_\alpha{}^{Y'}+\psi_\alpha{}^{Y'}\right)+tr\left(T_\alpha D_\alpha\right)+\\ \hat{c}_\alpha\theta_\alpha\eta_\alpha-\dfrac{q_\alpha\cdot g_\alpha}{\theta_\alpha}+\hat{e}_\alpha\end{matrix}\right\}\geq 0 \qquad (6)$$

In what follows, the temperature gradient, grad(θ_α), will be denoted by g_α, when the gradient is taken wrt the deformed coordinates. The Lagrangian counterpart will be denoted by GRAD(θ_α) = G_α.

It is assumed that there are no point sources in the mixture. This assumption requires the following:

$$\sum_{\alpha=1}^{N}\hat{c}_\alpha=0$$

$$\sum_{\alpha=1}^{N}\hat{p}_\alpha=0 \qquad (7)$$

$$\sum_{\alpha=1}^{N}\hat{e}_\alpha=0$$

In what follows, the independent variables will be taken to be the set (F_α, u_α, θ_α, G_α, X_α, ξ_α, l_α, t), while the dependent variables are assumed to be the set $\left(T_\alpha, q_\alpha, e_\alpha, \eta_\alpha, \psi_\alpha\right)$. The term l_α is called the extent of reaction and measures the extent to which the α^{th} constituent has gained or lost mass by chemical interaction or phase change. The dependent variables have the general form:

$$\begin{aligned}&\left(T_\alpha, q_\alpha, e_\alpha, \eta_\alpha, \psi_\alpha\right)(X,t)=\\ &f_\alpha\left(F_\alpha, u_\alpha, \theta_\alpha, G_\alpha, X_\alpha, \xi_\alpha, l_\alpha, t\right)\end{aligned} \qquad (8)$$

At the same time, dependence of interaction terms is assumed to have the general form:

$$\left(\hat{c}_\alpha, \hat{p}_\alpha, \hat{e}_\alpha\right)(X,t)=\hat{f}_\alpha\begin{pmatrix}F_\beta, u_\beta, \theta_\beta, G_\beta,\\ X_\beta, \xi_\beta, l_\beta, t\end{pmatrix}\quad \forall\,\beta\in[1,N] \qquad (9)$$

The procedures for developing the restrictions imposed by the second law are now well recognised[5]. Direct application of Eqn (6) gives the following results:

$$\tilde{T}_\alpha=\rho_\alpha\, det\left|F_\alpha\right|\frac{\partial\psi_\alpha}{\partial E_\alpha} \qquad (10)$$

$$\eta_\alpha=-\frac{\partial\psi_\alpha}{\partial\theta_\alpha} \qquad (11)$$

$$\frac{\partial\psi_\alpha}{\partial g_\alpha}=0 \qquad (12)$$

$$\frac{\partial\psi_\alpha}{\partial u_\alpha}=0 \qquad (13)$$

The second law can be reduced to:

$$\delta=\sum_{\alpha=1}^{N}\frac{1}{\theta_\alpha}\left\{-\rho_\alpha\frac{\partial\psi_\alpha}{\partial\xi_\alpha}\cdot\overset{Y}{\xi}_\alpha+\hat{e}_\alpha-\frac{q_\alpha\cdot g_\alpha}{\theta_\alpha}+\left[\theta_\alpha\eta_\alpha-\rho_\alpha\frac{\left|F_\alpha\right|}{\rho_{\alpha 0}}\frac{\partial\psi_\alpha}{\partial l'_\alpha}\right]\hat{c}_\alpha\right\}\geq 0 \qquad (14)$$

The term δ represents the value of entropy production. By defining thermomechanical equilibrium to be the state where all temperature gradients, interactions and velocities vanish, one can determine that the entropy production vanishes. One defines equilibrium to be the condition as

$$\left.\begin{aligned}&\theta_\alpha=\theta^e\\ &\overset{Y'}{\xi}{}^e_\alpha=0\\ &g^e_\alpha=0 \qquad \alpha=1,\ldots,N\\ &v^e_\alpha=0\\ &\hat{c}^e_\alpha=0\\ &\hat{e}^e_\alpha=0\end{aligned}\right\} \qquad (15)$$

Thermomechanical equilibrium essentially requires that when a material reaches an equilibrium state, the dissipation δ vanishes. Let s^e represents the set of variables in Eqn (15) at an equilibrium state, and let εs^p be an arbitrary perturbation away from this equilibrium state, where ε is an arbitrarily small scalar quantity, and s^p is an arbitrary vector perturbation in the independent variable vector. For any perturbation of the independent variables from an equilibrium state, one must have the following

restrictions:

$$\delta(s^e) = 0$$

$$\delta' = \delta(s^e + \varepsilon s^p) \geq 0 \qquad (16)$$

This condition implies:

$$\frac{d}{d\varepsilon}\delta(s^e + \varepsilon s^p)_{\delta=0} = 0$$

$$\frac{d^2}{d\varepsilon^2}\delta(s^e + \varepsilon s^p)_{\delta=0} \geq 0 \qquad (17)$$

These two relations collectively allows one to impose the following restrictions on the constitutive relations for each of the constituents:

$$\left[\rho_\beta \frac{\partial \psi_\beta}{\partial \xi_\beta} \cdot \frac{\partial \overset{Y'}{\xi}_\beta}{\partial \theta_\beta}\right]^e = 0, \quad \left[\sum (e_\alpha - \mu_\alpha)\frac{\partial \hat{c}_\alpha}{\partial \theta_\beta}\right]^e = 0 \quad \beta = 1, \ldots, N \qquad (18)$$

$$\left[\rho_\beta \frac{\partial \psi_\beta}{\partial \xi_\beta} \cdot \frac{\partial \overset{Y'}{\xi}_\beta}{\partial E_\beta}\right]^e = 0, \quad \left[\sum (e_\alpha - \mu_\alpha)\frac{\partial \hat{c}_\alpha}{\partial E_\beta}\right]^e = 0 \quad \beta = 1, \ldots, N$$

$$\left[\rho_\beta \frac{\partial \psi_\beta}{\partial \xi_\beta} \cdot \frac{\partial \overset{Y'}{\xi}_\beta}{\partial u_\beta}\right]^e = 0, \quad \left[\sum (e_\alpha - \mu_\alpha)\frac{\partial \hat{c}_\alpha}{\partial u_\beta}\right]^e = 0 \quad \beta = 1, \ldots, N$$

$$\left[\rho_\beta \frac{\partial \psi_\beta}{\partial \xi_\beta} \cdot \frac{\partial \overset{Y'}{\xi}_\beta}{\partial l_\beta}\right]^e = 0, \quad \left[\sum (e_\alpha - \mu_\alpha)\frac{\partial \hat{c}_\alpha}{\partial l_\beta}\right]^e = 0 \quad \beta = 1, \ldots, N$$

$$\left[\rho_\beta \frac{\partial \psi_\beta}{\partial \xi_\beta} \cdot \frac{\partial \overset{Y'}{\xi}_\beta}{\partial \xi_\beta}\right]^e = 0, \quad \left[\sum (e_\alpha - \mu_\alpha)\frac{\partial \hat{c}_\alpha}{\partial \xi_\beta}\right]^e = 0 \quad \beta = 1, \ldots, N \qquad (19)$$

$$q_\beta{}^e = 0, \quad \left[\sum (e_\alpha - \mu_\alpha)\frac{\partial \hat{c}_\alpha}{\partial u_\beta}\right]^e = 0 \quad \beta = 1, \ldots, N \qquad (20)$$

$$-\left[\frac{\partial^2 \rho_\alpha \psi_\alpha}{\partial E_{\alpha ij}\partial \xi_\alpha} \cdot \frac{\partial \overset{Y'}{\xi}_\alpha}{\partial E_{\alpha kl}}\right]^e + \left[\frac{\partial^2 \rho_\alpha \psi_\alpha}{\partial E_{\alpha kl}\partial \xi_\alpha} \cdot \frac{\partial \overset{Y'}{\xi}_\alpha}{\partial E_{\alpha ij}}\right]^e = 0 \quad (ij \neq kl) \qquad (21)$$

$$\left[\frac{\partial}{\partial E_{\alpha ij}}(e_\alpha - \mu_\alpha)\frac{\partial \hat{c}_\alpha}{E_{\alpha kl}}\right]^e + \left[\frac{\partial}{\partial E_{\alpha kl}}(e_\alpha - \mu_\alpha)\frac{\partial \hat{c}_\alpha}{E_{\alpha ij}}\right]^e = 0 \quad (ij \neq kl)$$

$$-\left[\frac{\partial^2 \rho_\alpha \psi_\alpha}{\partial E_{\alpha ij}\partial \xi_\alpha} \cdot \frac{\partial \overset{Y'}{\xi}_\alpha}{\partial E_{\alpha kl}}\right]^e + \left[\frac{\partial^2 \rho_\alpha \psi_\alpha}{\partial E_{\alpha kl}\partial \xi_\alpha} \cdot \frac{\partial \overset{Y'}{\xi}_\alpha}{\partial E_{\alpha ij}}\right]^e = 0 \quad (ij \neq kl) \qquad (22)$$

$$\left[\frac{\partial}{\partial E_{\alpha ij}}(e_\alpha - \mu_\alpha)\frac{\partial \hat{c}_\alpha}{E_{\alpha kl}}\right]^e + \left[\frac{\partial}{\partial E_{\alpha kl}}(e_\alpha - \mu_\alpha)\frac{\partial \hat{c}_\alpha}{E_{\alpha ij}}\right]^e = 0 \quad (ij = kl)$$

$$-\left[\frac{\partial^2 \rho_\alpha \psi_\alpha}{\partial E_{\alpha ij}\partial \xi_\alpha} \cdot \frac{\partial \overset{Y'}{\xi}_\alpha}{\partial E_{\alpha kl}}\right]^e + \left[\frac{\partial^2 \rho_\alpha \psi_\alpha}{\partial E_{\alpha kl}\partial \xi_\alpha} \cdot \frac{\partial \overset{Y'}{\xi}_\alpha}{\partial E_{\alpha ij}}\right]^e \geq 0 \quad (ij = kl) \qquad (23)$$

$$\left[\frac{\partial}{\partial E_{\alpha ij}}(e_\alpha - \mu_\alpha)\frac{\partial \hat{c}_\alpha}{E_{\alpha kl}}\right]^e + \left[\frac{\partial}{\partial E_{\alpha kl}}(e_\alpha - \mu_\alpha)\frac{\partial \hat{c}_\alpha}{E_{\alpha ij}}\right]^e \geq 0 \quad (ij = kl)$$

$$-\left[\frac{2}{\theta} \cdot \frac{\partial^2 \rho_\alpha \psi_\alpha}{\partial E_{\alpha ij}\partial \xi_\alpha} \cdot \frac{\partial \overset{Y'}{\xi}_\alpha}{\partial E_{\alpha kl}}\right]^e \leq 0 \quad \theta_\alpha^p \neq 0, \quad \theta_\beta^p = 0 \qquad (24)$$

$$\left[-\frac{1}{\theta_\alpha^2}\frac{\partial \hat{e}_\alpha}{\partial \theta_\beta}+\frac{2}{\theta_\alpha}\frac{\partial}{\partial \theta_\alpha}(e_\alpha-\mu_\alpha)\frac{\partial \hat{c}_\alpha}{\partial \theta_\beta}\right]^e$$

$$=0 \qquad \alpha\neq\beta,\ \theta_\alpha^p\neq 0,\ \theta_\beta^p\neq 0$$

$$\left[-\frac{1}{\theta_\alpha^2}\frac{\partial \hat{e}_\alpha}{\partial \theta_\beta}-\frac{2}{\theta}\frac{\partial}{\partial \theta_\alpha}(e_\alpha-\mu_\alpha)\frac{\partial \hat{c}_\alpha}{\partial \theta_\beta}\right]^e$$

$$=0 \qquad \alpha\neq\beta,\ \theta_\alpha^p\neq 0,\ \theta_\beta^p\neq 0 \qquad (25)$$

$$\left[-\frac{1}{\theta_\alpha^2}\frac{\partial \hat{e}_\alpha}{\partial \theta_\beta}-\frac{2}{\theta_\alpha}\frac{\partial^2 \rho_\alpha \psi_\alpha}{\partial \theta_\alpha \partial \xi_\alpha}\cdot\frac{\partial \overset{Y'}{\xi}_\alpha}{\partial \theta_\alpha}+\frac{2}{\theta_\alpha}\frac{\partial}{\partial \theta_\alpha}\right.$$
$$\left.(e_\alpha-\mu_\alpha)\frac{\partial \hat{c}_\alpha}{\partial \theta_\alpha}-\frac{\partial}{\partial \theta_\alpha}\left(\frac{q_\alpha}{\theta_\alpha}\right)\cdot\frac{\partial g_\alpha}{\partial \theta_\beta}\right]^e$$

$$\geq 0 \qquad \alpha=\beta,\theta_\alpha^p\neq 0 \qquad (26)$$

$$\left[\frac{\partial q_\alpha}{\partial g_\alpha}\right]^e\leq 0 \qquad (27)$$

By observing Eqns (18)-(26), one can see that the expression $(\varepsilon_\alpha-\mu_\alpha)$ is a central feature of the restrictions imposed by the second law. This difference between the internal energy (ε_α) and the chemical potential (μ_α) is denoted by Δ_α and will be referred to as the potential difference.

$$\Delta_\alpha=(e_\alpha-\mu_\alpha) \qquad (28)$$

The chemical potential[6] is given by the expression

$$\mu_\alpha=\frac{\partial}{l_\alpha}(l_\alpha\psi_\alpha)=\frac{\partial}{\rho_\alpha}(\rho_\alpha\psi_\alpha) \qquad (29)$$

The extent of reaction l_α provides a measure of the interchange of mass that has occurred between the α^{th} constituent and the other $(N-1)$ constituents. The extent of reactions is defined to have the form:

$$l_\alpha=\frac{\rho_\alpha}{\rho_{\alpha R}}det|F_\alpha| \qquad (30)$$

where $\rho_{\alpha R}$ is the initial dispersed density of the α^{th} constituent. The extent of reaction reflects how much mass the α^{th} constituent has lost or gained from the other phases due to chemical reactions and/or phase changes. The determinant of the deformation gradient reflects how the density changes due to deformation processes. For instance, if there is no net gain or loss of mass due to chemical interaction of the α^{th} constituent with the other constituents, the density obeys the relation $\rho_{\alpha R}|\rho_\alpha=det|F_\alpha|$. Therefore, if there is no mass exchange, l_α will remain unity, as determined by Eqn (30). Any change from unity implies the relative change in density due to chemical interactions. The time rate of change is given by the expression:

$$\overset{Y'}{l}_{\alpha_{\dot{\alpha}}}=\frac{det|F_\alpha|}{\rho_{\alpha R}}\hat{c}_\alpha \qquad (31)$$

The potential difference Δ_α can be shown to have the form:

$$\Delta_\alpha=-\left(\theta_\alpha\frac{\partial \psi_\alpha}{\partial \theta_\alpha}+l_\alpha\frac{\partial \psi_\alpha}{\partial l_\alpha}\right) \qquad (32)$$

so that Δ_α is completely expressible in terms of free energy.

3. APPLICATION TO EQUITEMPERATURE METAMORPHISM OF SNOW

The material is now represented as a collection of constituents consisting of ice grains and/or intergranular necks with specific geometries, an air phase and a vapour phase. The last two constituents occupy the pore space in this bonded granular material. Each ice grain constituent will be identified as having a grain size (r_α). α denotes an ice grain constituent $(\alpha=1,...N)$. Each of the neck constituents will also be identified by its geometry which in this case will be the bond radius, $(r_{b\alpha})$, where b will denote a neck to differentiate between a neck property and a grain property. Each neck will have its own length, $l_{b\alpha}$, which is determined by the size of the bond radius and the radius of the grain to which it is attached. The vapour and air phases will be denoted by the subscripts v and a, respectively. Therefore, the mixture is considered to be composed of a set of ice grains with specified initial sizes, intergranular necks with specified initial sizes, a

vapour phase and an air phase. The grain and neck dispersed densities are denoted by r_α and $r_{b\alpha}$, respectively. For this particular problem, it is assumed that no external loads are applied, no temperature gradient exist and that only the slow, steady process of redistribution of mass within the material is taking place due to differences in surface energy of various constituents. The purpose is the evaluation of many details relating to changes in microstructure during this important thermomechanical process.

Helmholtz free energy for each of constituent is the central function. In this study, the free energies are represented by second-order Taylor series expansions and the relations presented in the preceeding section are used to write the constitutive relations. The free energy expansions for the ice constituents are:

$$\begin{aligned}\psi_\alpha &= \psi_{\alpha 0} + \psi_{\alpha 1}(trE_\alpha) + \psi_{\alpha 2}(\theta_\alpha - \theta_R) \\ &+ \psi_{\alpha 3}(l_\alpha - l_R) + \frac{1}{2}\Big[\psi_{\alpha 4}(trE_\alpha)^2 + \psi_{\alpha 5} \\ &\times (trE_\alpha^2) + 2\psi_{\alpha 6}(\theta_\alpha - \theta_R)trE_\alpha \\ &+ \psi_{\alpha 7}(\theta_\alpha - \theta_R)^2 + 2\psi_{\alpha 8}(\theta_\alpha - \theta_R)(l_\alpha - l_R) \\ &+ 2\psi_{\alpha 9}(l_\alpha - l_R)trE_\alpha + \psi_{\alpha 10}(l_\alpha - l_R)^2\ \Big]\end{aligned} \tag{33}$$

The coefficients $\psi_{\alpha 0}$, ..., $\psi_{\alpha 10}$ can be shown to have the forms:

$$\begin{aligned}&\psi_{\alpha 0} = \frac{2\sigma_s}{\gamma_i r_{\alpha R}}, \qquad \psi_{\alpha 1} = \frac{\sigma_0}{\rho_{\alpha R}}, \\ &\psi_{\alpha 2} = -\eta_{\alpha R}, \qquad \psi_{\alpha 3} = -\frac{\sigma_s}{9\gamma_i r_{\alpha R}}, \\ &\psi_{\alpha 4} = \frac{\lambda}{\rho_{\alpha R}}, \qquad \psi_{\alpha 5} = \frac{\mu}{\rho_{\alpha R}}, \\ &\psi_{\alpha 6} = \frac{\alpha(3\lambda + 2\mu)}{\rho_{\alpha R}}, \qquad \psi_{\alpha 7} = -\frac{2C_{i\theta}}{\theta_R}, \\ &\psi_{\alpha 8} = \psi_{\alpha 10} = 0, \qquad \psi_{\alpha 9} = \sigma_{0\alpha}\end{aligned} \tag{34}$$

The term γ_i is the density of ice (917 kg/m^3). The free energy for the vapour is:

$$\begin{aligned}\psi_v &= \psi_{v0} + \psi_{v1}(\theta_v - \theta_R) + \psi_{v2}(\rho_v - \rho_{vR}) + \psi_{v3}(l_v - l_{vR}) \\ &+ \frac{1}{2}\Big[2\psi_{v4}(\theta_v - \theta_R)(\rho_v - \rho_{vR}) + 2\psi_{v5}(\theta_v - \theta_R)(l_v - l_{vR}) \\ &+ \Big[2\psi_{v6}(l_v - l_{vR})(\rho_v - \rho_{vR}) + \psi_{v7}(\theta_v - \theta_R)^2 \\ &+ \psi_{v8}(\rho_v - \rho_{vR})^2 + \psi_{v9}(l_v - l_{vR})^2\Big]\end{aligned} \tag{35}$$

With the coefficients ψ_{v0}, ..., ψ_{v10} having the values:

$$\left.\begin{aligned}&\psi_{v1} = -\eta_{vR}, \qquad \psi_{v2} = \frac{R\theta_R}{\rho_{vR}} \\ &\psi_{v3} = R\theta_R, \qquad \psi_{v4} = \frac{R}{\rho_{vR}} \\ &\psi_{v5} = R, \qquad \psi_{v6} = \frac{R\theta_R}{\rho_{vR}} \\ &\psi_{v7} = \frac{C_v}{\theta_R}, \qquad \psi_{v8} = \frac{R\theta_R}{\rho^2{}_{vR}} \\ &\psi_{v9} = -R\theta_R\end{aligned}\right\} \tag{36}$$

The constitutive relation for the vapour as determined by Eqn (10) becomes:

$$\begin{aligned}T_v &= -\rho_v^2\left[\frac{R\theta_R}{\rho_{vR}} + \frac{R}{\rho_{vR}}(\theta_v - \theta_R) + \frac{R\theta_R}{\rho_{vR}}(l_v - l_{vR})\right. \\ &\left. + \frac{R\theta_R}{\rho_{vR}^2}(\rho_v - \rho_{vR})\right]I \\ &= \frac{\rho_v^2 R}{\rho_{vR}}\left[\theta_v + \theta_R(l_v - l_{vR}) - \frac{\theta_R}{\rho_{vR}}(\rho_v - \rho_{vR})\right]I\end{aligned} \tag{37}$$

This constitutive relation for the vapour can be shown to represent the behaviour of a compressible ideal fluid. The constitutive relation for the ice constituents becomes:

$$\begin{aligned}\tilde{T}_\alpha &= det|F_\alpha|\{\sigma_{0\alpha}l_\alpha I + \lambda_\alpha(trE_\alpha)I + 2\mu_\alpha E_\alpha \\ &+ \alpha_\alpha(3\lambda_\alpha + 2\mu_\alpha)(\theta_\alpha - \theta_R)I\}\end{aligned} \tag{38}$$

The coefficients λ_α and μ_α are the usual Lame constants for a linear elastic material and α_α is the coefficient of thermal expansion. For small deformations, the determinant of the deformation gradient for each ice constituent is approximately equal to unity, so that Piola stress is closely approximated by Cauchy stress. The term $\sigma_{0\alpha}$ is an internal initial stress that is generated by the surface tension within the material.

The mass interactions can be shown to have the forms:

$$\left.\begin{aligned} \hat{c}_\alpha &= m_{\alpha v}(\Delta_v - \Delta_\alpha),\ \alpha = 1,\ldots,N \\ \hat{c}_v &= -\sum_{\alpha=1}^{N} m_{\alpha v}(\Delta_v - \Delta_\alpha) \\ \hat{c}_\alpha &= 0 \end{aligned}\right\} \tag{39}$$

These potential differences then govern the rate at which mass exchanges take place. The above expression is a direct result of the restrictions imposed by the second law of thermodynamics and, therefore, will be observed.

By examining Eqn (39), one can see that each ice constituent is assumed to exchange mass only with the vapour phase, while the vapour phase can exchange mass simultaneously with all ice constituents. This assumption is a realistic one, since mass is sublimated off an ice surface into the pore space occupied by the vapour, while other grains may be acquiring mass by having vapour condensed onto their ice surfaces. It is, therefore, the vapour phase that indirectly provides for mass leaving one ice surface and eventually being deposited upon another ice surface. This representation of the mass interaction process precludes transfer of mass from one grain directly to another by volume diffusion or surface diffusion through the necks from one grain to another. Maeno and ebinuma[15] demonstrated that vapour diffusion dominates most situations.

The energy exchange is assumed to have the form:

$$\left.\begin{aligned} \hat{e}_\alpha &= K_{\alpha v}(\theta_v - \theta_\alpha) \\ \hat{e}_v &= -\sum_{\alpha=1}^{N} K_{\alpha v}(\theta_v - \theta_\alpha) \end{aligned}\right\} \tag{40}$$

This is a form similar to that used earlier by Adams and Brown[8] and is essentially Newton's law of cooling and will account for the interchange of thermal energy between constituents. Here, the direct interchange of energy between ice grains was neglected and it was assumed that energy is interchanged directly between the ice constituents and the vapour phase. This is reasonable if the intergranular bonding is typical for snow of low-to-medium density. For such snow, the intergranular bonds are often less than one half the grain radius, so the necks represent a severe constriction which negatively affects conduction of heat between grains. One can verify that the second law of thermodynamics is satisfied by Eqns (39) and (40).

The balance equations shown in Eqns (3)–(5) reduce to simplified forms, since the velocities, temperature gradient and heat conduction vanish. These simplified forms are then solved after substituting for the constitutive relations to determine the rates at which the constituents exchange mass. Before doing this, one needs to specify the geometry and the microstructure that will be used to study metamorphism.

4. SPECIFICATION OF MICROSTRUCTURE

The microstructure of the material determines the nature of metamorphism of snow under equitemperature conditions. Consider first how the microstructure affects the deformation and internal stresses. It is well understood that the surface tension in the ice grains will attempt to compress the material to a higher density to reduce the surface energy within the material. One starts by considering the special case when the strain is maintained at zero and the stress that must be developed within the material to keep $E_\alpha = 0$. Equation (38) gives the following value for the stress tensor, if there are no deformations, temperature changes or mass exchanges.

$$\tilde{T}_\alpha = \sigma_{0\alpha} l_\alpha I \tag{41}$$

Piola stress will approximate Cauchy stress whenever deformations are small. In this case, they will be equal, since strains are held at zero. Also, the extents of reaction (l_α), will have initial values

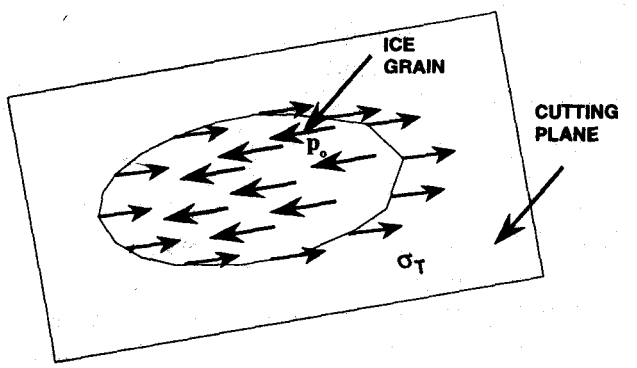

Figure 1. Inner surface of an ice grain exposed by a cutting plane through grain.

of unity but will change as the constituents exchange mass.

Figure1 illustrates conceptually the internal stresses within the ice grains that will be developed due to surface tension on each grain. If the internal stress must balance the surface tension (σ_T), one must have for the internal stress ($p_{0\alpha}$) within each ice grain:

$$p_{0\alpha} = \frac{2\sigma_T}{r_\alpha} \tag{42}$$

Assuming homogeneous and isotropic microstructure, surface fractions on any plane cut through a material are proportional to the mass fractions. One can then verify that $\sigma_{0\alpha} = (\rho_\alpha / \rho) p_{0\alpha}$, so that

$$\sigma_{0\alpha} = \frac{2\rho_\alpha \sigma_T}{\rho r_\alpha} \tag{43}$$

The free energy, entropy, chemical potential and internal energy are all reckoned per unit mass, whereas the surface energy (σ_s) is reckoned per unit area of ice surface. Let $\sum_{i\alpha}$ be the surface energy per unit mass, then, an approximate relation:

$$\sigma_s(4\pi r^2) = \sum_{is}\left(\frac{4}{3}\pi r_\alpha^3 \gamma_i\right) \tag{44}$$

where γ_i is the mass density of ice. One can show that in the reference configuration, one has

$$(\Delta_v - \Delta_\alpha)_R = \frac{\sigma_s}{4\gamma_i r_{\alpha R}} \tag{45}$$

for the difference between the potential differences for the vapour and the α^{th} ice constituent. Therefore, in the reference configuration one will have mass exchanges taking place, since the potential differences Δ_v and Δ_α are not equal. What will happen is that one starts with an initial state consisting of a collection of ice grains of different sizes and a vapour phase, the ice grains will lose mass to the vapour until its energy begins to exceed the energies of some of the ice grains. Then the vapour will begin to supply mass to grains with lower energies, while the grains with higher energies will continue to lose mass to the vapour. The vapour will reach a stable configuration with an energy level where it is continuously acquiring mass from some grains while at the same time giving up mass to other grains.

To characterise the geometry of the necks, consider two ice grains in direct contact with each other, as shown in Fig. 2. In this figure, the neck will have two surface curvature $r_{b\alpha}$ and $r_{c\alpha}$, where $r_{b\alpha}$ is the positive radius of curvature describing the

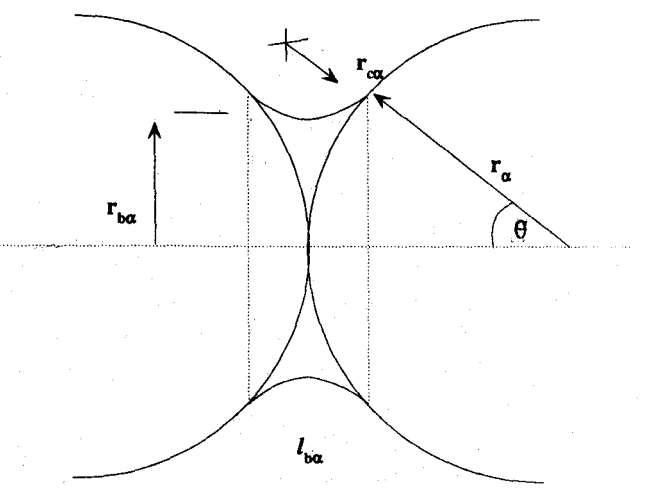

Figure 2. Basic neck geometry

bond radius. The other curvature, $r_{c\alpha}$, is the concave curvature seen in the figure and forms even in the absence of pressure sintering due to vapour diffusion to the neck. The concave radius (r_c) will always represent negative curvature, but is given a positive algebraic value. Therefore, the mean or effective curvature ($r_{n\alpha}$) of the neck is given by the following relation, where the minus sign reflects the negative curvature:

$$\frac{2}{r_\alpha} = \frac{1}{r_\alpha} - \frac{1}{r_{c\alpha}} \tag{46}$$

As can be seen, the concave radius ($r_{c\alpha}$) is determined by the requirement that the neck surface be asymptotic to the grain curvature. The ends of the neck are determined by the point on the ice surface where the surface curvature goes from a concave outward to a convex curvature. The neck length is denoted by $l_{b\alpha}$ (later by l_α), which is always positive. From Fig. 2, the following relations can be found:

$$l_{b\alpha} = \frac{2r_\alpha r_{c\alpha}}{r_\alpha + r_{c\alpha}}$$
$$r_{c\alpha} = \frac{r_{b\alpha}^2}{2(r_\alpha - r_{b\alpha})} \tag{47}$$

The surface area of the neck will be approximated by the following relation:

$$\sum\nolimits_n = 2\pi r_{b\alpha} l_\alpha \tag{48}$$

An important factor that determines how rapidly the various ice constituents interchange mass is the free surface area (S_α). These values are determined by the density and the radii of curvature. Approximate values can be found from the relations:

$$S_\alpha = \frac{3\rho_\alpha}{\gamma_i r_\alpha}, \quad \textit{grains}$$
$$S_\alpha = \frac{3\rho_{b\alpha}}{\gamma_i r_{b\alpha}}, \quad \textit{necks} \tag{49}$$

The density of the necks is determined by both the neck size and the three-dimensional coordination number, $N_{\alpha 3}$, which gives the mean number of bonds per grain. The coefficients $m_{\alpha v}$ and $K_{\alpha v}$ in Eqns (39) and (40), respectively, for the mass and energy exchanges are assumed to depend on the free surface area and the equilibrium vapour density for the surface. This is determined by the surface curvature and the temperature. The relation adopted is:

$$m_{\alpha v} = c_0 S_\alpha e^{\left[2\sigma/(\gamma_i R\theta_\alpha r_\alpha)\right]} e^{\left[(L/R)(1/\theta_T - 1/\theta_\alpha)\right]} \tag{50}$$

$$K_{\alpha v} = K_0 S_\alpha e^{\left[2\sigma/(\gamma_i R\theta_\alpha r_\alpha)\right]} e^{\left[(L/R)(1/\theta_T - 1/\theta_\alpha)\right]} \tag{51}$$

In these two equations, the radius r is either the grain radius (r_α) or the neck effective radius ($r_{n\alpha}$), depending on whether the constituent is a grain or a neck. The exponential terms reflect the dependence of equilibrium vapour pressure on surface curvature and temperature. In above relations, L is the latent heat of sublimation; σ, the surface energy; and R, the universal gas constant. These coefficients reflect the fact that mass and energy exchanges are facilited by the availability of free surface area and vapour available at the surface for exchange of mass and energy.

5. APPLICATION

Several examples are considered to have some insight into the process of equitemperature metamorphism and to demonstrate the formulation. The governing equations are solved numerically by a standard numerical integration procedure. Since metamorphism can result in large changes in the mass density of the constituents, Taylor series expansions of the constitutive relations cannot be considered to remain valid over the entire integration period. Consequently, whenever any constituent density was changed by more than 1 per cent of its original density, the reference configuration was updated to the current configuration, the Taylor coefficients were recalculated, and the integration process was then restarted.

5.1 Material with Five Grain Sizes & Five Neck Sizes

As a first application of the theory, grain size distribution is approximated by five discrete grain sizes. It is assumed that initially all five grain sizes, each considered to be a constituent, have the same initial number densities (number of grains per unit volume). In addition, it is assumed that the ice grains are interconnected by a distribution of necks with bond radii which equal 10 per cent of the grain radii. This would represent a material with a weak initial intergranular bonding. The purpose is to then determine the time-dependent growth of the bond and grain size distribution. Information relevant to this problem is given in Table 1. The three-dimensional coordination number N_3 (number

Table 1. Microstructure

Grains constituent No.	Grain size (mm)	Density (kg/m^3)	Free surface area (m^{-1})	Number density (m^{-3})
1	5.0000	2.00×10^{2}	1.31×10^{2}	4.2×10^{5}
2	2.5000	2.50×10^{1}	3.27×10	4.2×10^{5}
3	1.0000	1.60×10^{0}	5.23×10^{0}	4.2×10^{5}
4	0.5000	2.00×10^{-1}	1.31×10^{0}	4.2×10^{5}
5	0.2500	2.50×10^{-3}	3.27×10^{-1}	4.2×10^{5}
6	0.5000	3.56×10^{-2}	1.59×10^{-1}	1.05×10^{6}
7	0.2500	4.56×10^{-3}	3.98×10^{-2}	1.05×10^{6}
8	0.1000	2.92×10^{-4}	6.36×10^{-3}	1.05×10^{6}
9	0.0500	3.65×10^{-5}	1.59×10^{-3}	1.05×10^{6}
10	0.0250	4.56×10^{-6}	3.98×10^{-4}	1.05×10^{6}

of bonds/grain) is assumed to have a value of 2.50, so that the number of bonds is 250 per cent the number of grains. A value of 2.50 is slightly higher than what has been measured[16] for snow with densities of approx. 250 kg/m^3. Since each constituent has approx. 420,000 grains per cu meter each neck constituent will have 1, 050,000 grains per cu meter.

The size distribution could have been so chosen that each grain size had equal dispersed densities (ρ_α), or grain size with a log normal distribution could have been chosen. Until quantitative stereology methods are used to make accurate determinations of grain and neck size distributions, ideal models, such as above will have to be used. Recent results indicate that progress in quantitative stereology may soon yield the ability to accurately determine these distributions.

The mass, momentum and energy balance relations are solved to find the changes in constituent densities and temperatures with time. The initial temperature was set at -10 °C, but the constituent temperatures will not be discussed, since changes in constituent temperatures were so small as to not be of interest. Only the interchange of mass between the ten constituents (five grain constituents and five neck constituents) has been discussed here. The balance equations were solved numerically after substituting the appropriate constitutive relations into these equations. The results obtained are demonstrated in Figs 3-5.

As may be observed, the smallest grains lose mass fairly rapidly. The smallest-grained constituent is almost eliminated by the end of 30 days. The largest-grained constituent gains mass very slowly, while the other four lose mass, the rate of mass loss increasing with decreasing size. After the two smallest constituents are eliminated, the process becomes very slow.

Time-dependent changes in bond size for the neck constituents are depicted in Fig. 4. The smallest necks (constituent No. 10) grow very quickly until about 10 days, after which the growth rate decreases; it begins to decrease dramatically after the twentieth

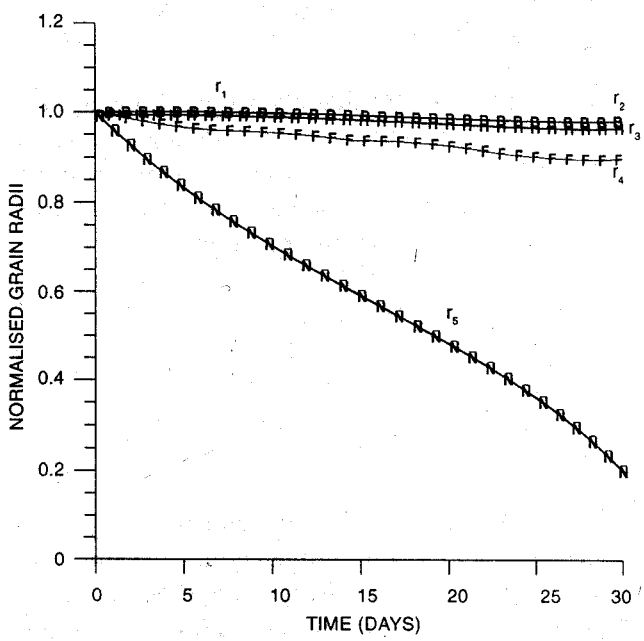

Figure 3. Variation of grain size for case where grains are bonded by necks with bond radii equaling 10 per cent the grain radii.

day. These are the necks which interconnect the smallest grains (constituent No. 5). These necks begin losing mass, because they are overtaking their grains in size, and their geometry changes so that their surface energies begin to exceed those of some of the other ice constituents and hence their subsequent loss of mass. However, they still continue to grow relative to the grains to which they are attached.

The variation of bond/grain size is depicted in Fig.5. As can be seen, the bonds demonstrate considerable sintering with time. The smallest grain/neck combination is of particular interest. The ratio r_b/r_a for this combination (constituent Nos. 10 and

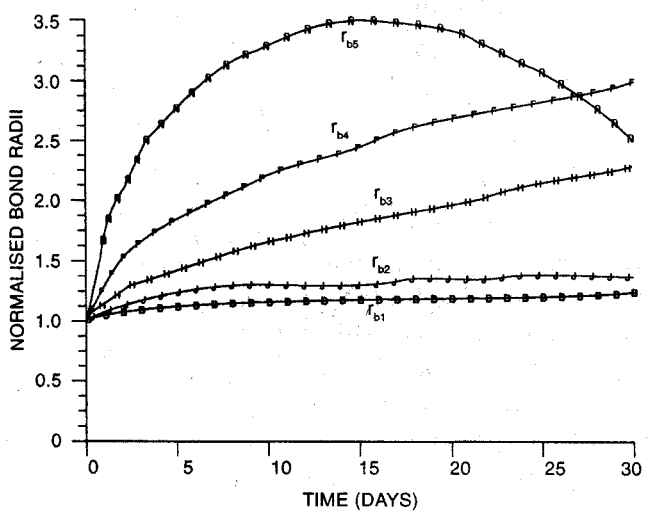

Figure 4. Variation of bond dimensions with time

5) shows that the bond radius exceeds the grain radius as the thirtieth day is approached. By this time, the fifth grain constituent is essentially eliminated, and two grains interconnected by a bond have for all practical purposes merged into one grain due to growth of the neck connecting these two grains. Equation (46) may be used to show that the effective radius is still larger than the grain radius even when bond radius r_b reaches the value of the grain radius r_g. At this point, r_c becomes infinite and one has $r_n = 2r_g$, so that the effective curvature of the neck is still larger than that of the grain. Consequently, the neck will lose mass more slowly than the grains that it interconnects. The two grains will merge into one grain. But in this case, by the time this

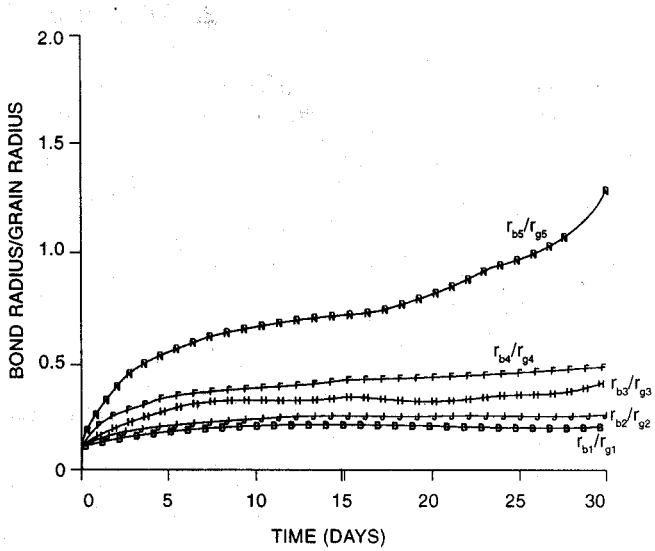

Figure 5. Variation with time of ratio of bond radii to grain radii.

occurrs, they are practically eliminated.

5.2 Effect of Mean Grain Size

As another example, the case where the snow is modelled as a mixture of five grain sizes was considered, but this time the presence of intergranular necks was not included. In addition, it was assumed that the initial grain distribution is such that all grain sizes have equal initial mass densities (ρ_α) of 50 kg/m^3. As an added feature, the rates at which metamorphism proceeds were compared for two different snows, one large-grained and the other small-grained. The large-grained snow was assumed to have a size distribution which is ten times as large as that of the fine-grained snow. The grain size for the five constituents in the fine-grained snow was assumed to be 0.025, 0.05, 0.1, 0.25 and 0.50 mm, while the large-grained snow had a size distribution 0.25, 0.5, 1.0, 2.5 and 5.0 mm. Obviously, the free surface area available for mass exchanges was much larger for the fine-grained snow, and hence one would expect the redistribution of grain sizes to proceed much more rapidly in fine-grained snow. The relevant physical properties for the two materials are presented in Tables 2 and 3.

The relative rates of metamorphism for the large-grained snow and the fine-grained snow have

Table 2. Microstructure for large-grained snow

Grains constituent No.	Grain size (mm)	Density (kg/m^3)	Free surface area (m^{-1})	Number density (m^{-3})
1	5.00	50.0	3.27×10^2	1.0×10^6
2	2.50	50.0	6.54×10^2	8.3×10^6
3	1.00	50.0	1.64×10^3	1.3×10^8
4	0.50	50.0	3.27×10^3	1.0×10^9
5	0.25	50.0	6.54×10^3	8.3×10^9

Table 3. Microstructure for fine-grained snow

Grains constituent No.	Grain size (mm)	Density (kg/m^3)	Free surface Area (m^{-1})	Number density (m^{-3})
1	0.50	50.0	3.27×10^3	1.0×10^8
2	0.25	50.0	6.54×10^3	8.3×10^8
3	0.1	50.0	1.64×10^4	1.3×10^{10}
4	0.05	50.0	3.27×10^4	1.0×10^{11}
5	0.025	50.0	6.54×10^4	8.3×10^{11}

been illustrated in Fig 6. The figure depicts density distribution for the two types of snow at four given times. The horizontal axis represents the initial grain sizes, though it must be kept in mind that the initial dimensions for the two types of snow differ by a factor of 10. The first figure shows the distribution at the initial time when all constituents have densities of 50 kg/m^3. By 30 days, the two smallest constituents in the fine-grained snow have completely disappeared. In contrast, the large-grained snow has gone though a relatively minor change in grain size distribution. The remaining two parts of the figure are for 60 and 90 days.

One can see that the nature of metamorphism is different from that in the first example for both large-grained and fine-grained snow. In this example, the second smallest-grained constituent actually gains mass for some time as opposed to the first example. In the first example, where all constituents had equal number of densities (N_α), the largest-grained constituent extracted mass from all the smaller grains, with the result that all these constituents lost mass. In this example, where all constituents have equal initial mass densities, it was seen that the surface areas of the small-grained constituents are much larger than that of constituent No. 5, and this is responsible for the two smallest constituents interacting with each other. Constituent No. 5 is sacrificed in favour of Constituent No. 2, which gains mass until the smaller one is nearly depleted. Then this constituent begins losing mass to the next larger one.

5.3 Effect of Temperature

Temperature naturally plays a role in the rate at which any form of metamorphism progresses. This is seen in the effect that temperature has on the free energy and on the potential differences Δ_v. Calculations were carried out for four temperatures, −5, −10, −20 and −70° C. In this example, one considers the five grain size to be 0.25, 0.5, 1.0, 2.5 and 5.0 mm. Each grain size was assumed to have an initial density of 50 kg/m^3. The relative changes in the grain size constituent densities for these initial grain sizes are demonstrated in Fig. 7.

The temperatures of −5 °C and −10 °C are characteristic of the temperatures that would exist in seasonal snow cover in the alpine areas of the

United States. The lowest temperature shown here, –70 °C, is characteristic of the temperatures that can be found in Antarctica during winter. Consequently, these rates of metamorphism would be relevant to processed snow that would be used for landing strips at the South Pole Station or other areas in the Antarctica. Note that the temperature is extremely important in determining the rate at which metamorphism advances. At –70 °C, the process is practically stopped.

5.4 Effect of Initial Grain Size Distribution

As indicated earlier, initial grain size can have an effect on the rate of metamorphism. To investigate this, two initial grain size distribution were considered. The first one was snow in which the grain size was evenly distributed wrt density, and the second one had a distribution approaching a normal distribution. Both materials had an initial mean grain size of 0.5 mm.

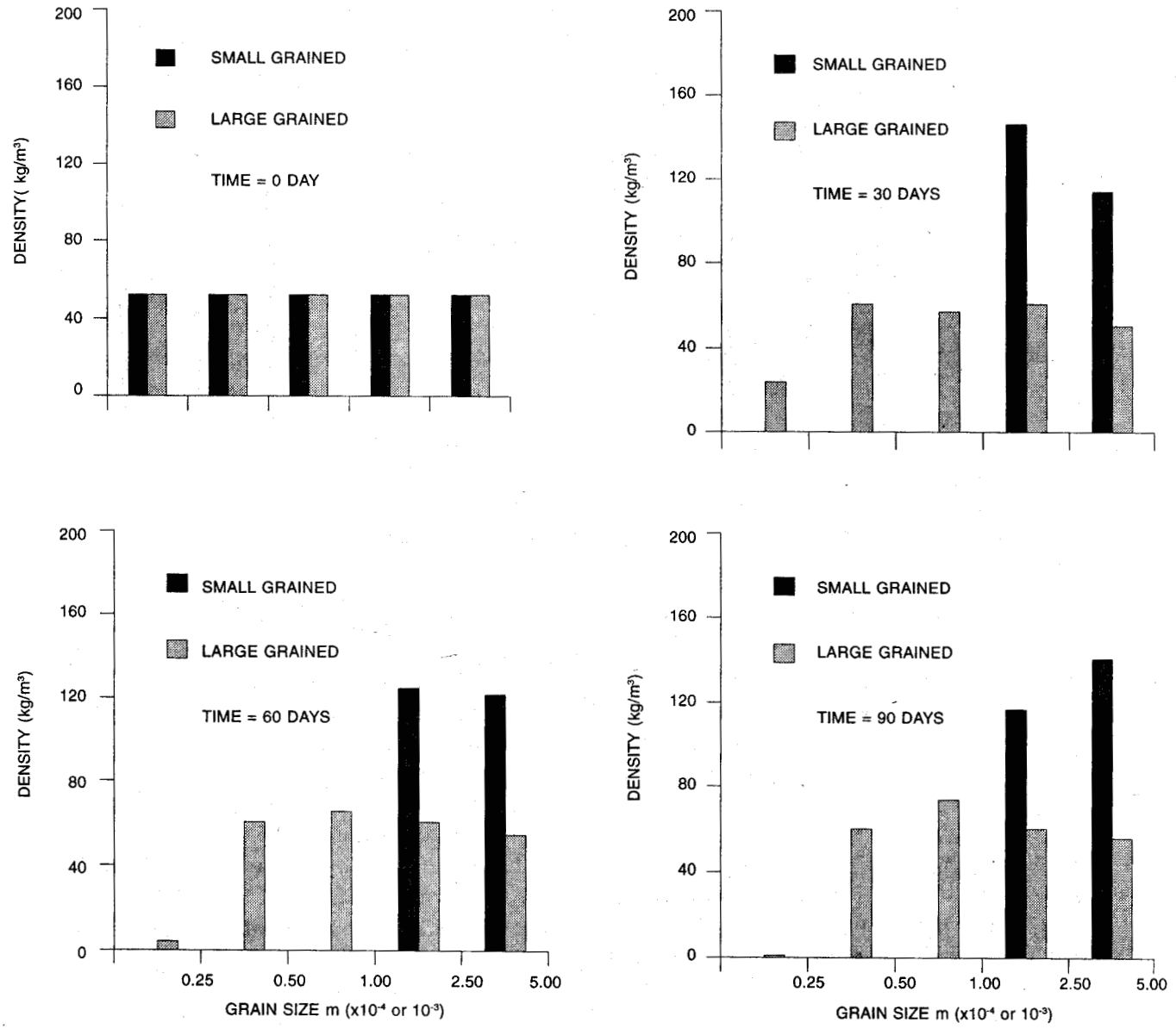

Figure 6. **Variation of density distribution of constituents with time. The fine-grained snow has an initial grain size distribution ranging from 0.025 mm to 0.5 mm. The large-grained snow has a distribution ranging from 0.25 mm to 5.0 mm, so that each constituent is 10 times as large as in the small-grained snow.**

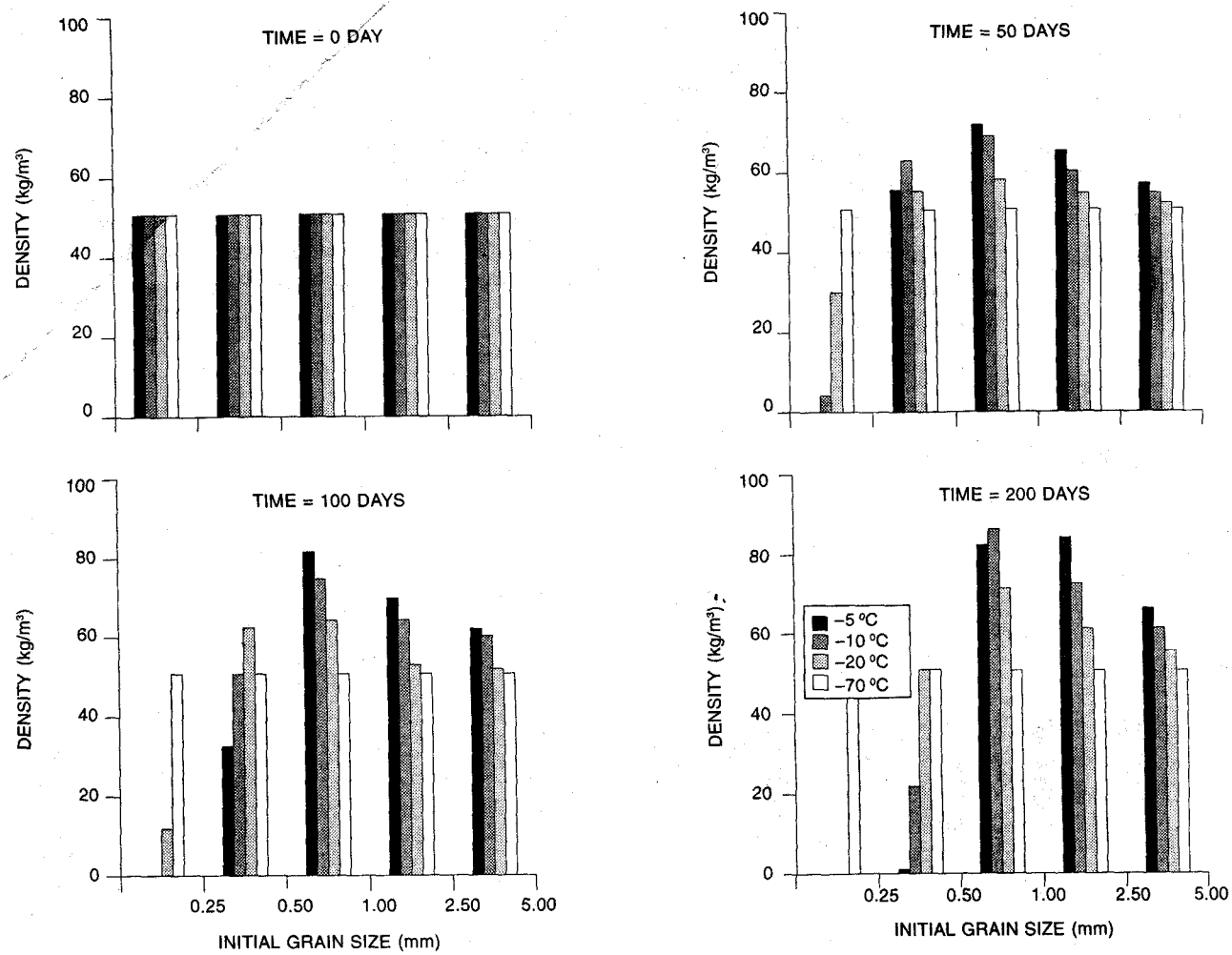

Figure 7. Effect of temperature upon rate of metamorphism

The time-dependent variation of grain size distribution for the two snow samples over a period of two years as calculated by the physical model presented here is depicted in Fig. 8. As one can see, the distribution does evolve towards a larger grain size distribution. The smaller grains are sacrificed in favour of the larger grains. By one year, grains with initial sizes smaller than 0.4 mm have been eliminated. However this does not imply that grains with smaller sizes will not exist within the material at any given time. Density distribution in terms of initial grain size instead of instantaneous size in depicted in Fig. 9. One should keep in mind that at any given time, the instantaneous grain size will generally be different from the initial grain size.

As can be seen in Fig. 8, grain size distribution are considerably different in their initial state, but they begin to acquire similar characteristics as time passes. To make a better comparison, variation of the mean grain size with time was considered. How these two materials change their mean grain size with time, is demonstrated in Fig. 9. An interesting result is that while the grain size distribution during the first 100 days are substantially different, the rates at which the two materials change also differ significantly, as implied by the slopes of the curves in Fig. 9. However, by 100 days, grain size distribution are somewhat similar (Fig. 8), and the rate of grain growth for the two materials approach each other.

6. CONCLUSION

In this paper, a mixture theory based on volume-fraction principle and utilising material microstructure has been developed and examined to determine if

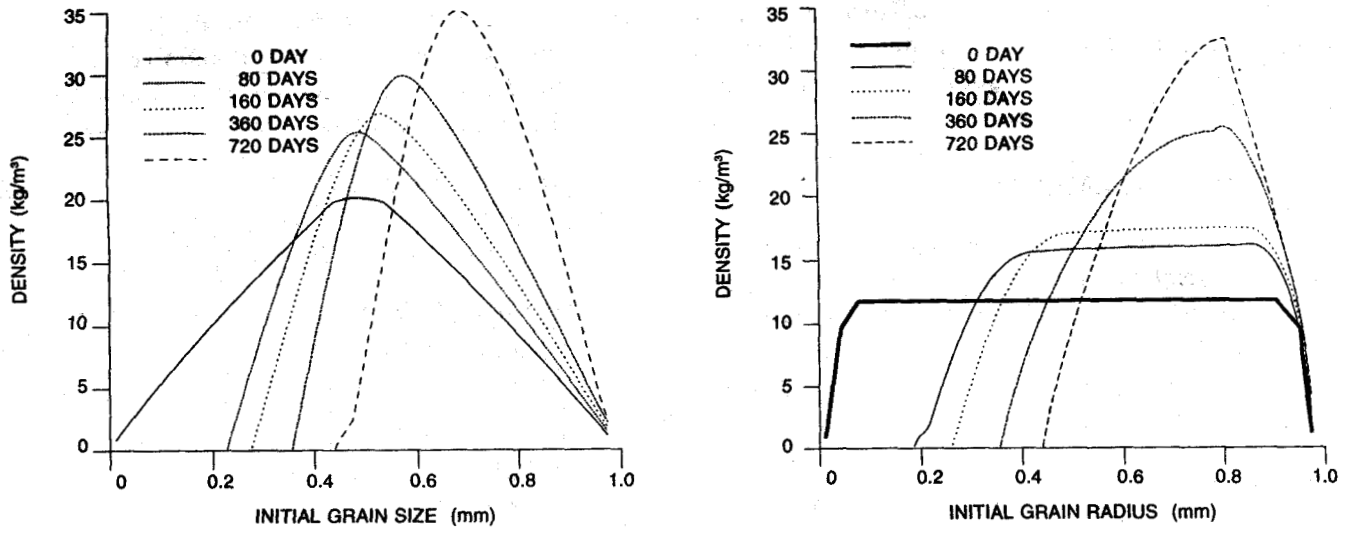

Figure 8. Comparison of grain size distribution evolution for two snow samples, one with a nearly uniform initial distribution, and the other with a more normal distribution.

such formulations can be put to use to predict heat and mass transfer in snow and firn. While experimental data to validate and calibrate such a theory is still being developed, the results do indicate that such mixture theories can be effectively used to predict material response to thermomechanical processes, such as metamorphism.

The examples given here demonstrate that if such formulations are to be used, an accurate description of the material microstructure is needed. The first example showed that under equi–temperature conditions, a complicated mass transfer process takes place with large grains acquiring mass from small grains and with the necks acquiring mass from all the grains. This was the situation for size distribution based on initial number densities for all constituents. However, if the initial microstructure had all constituents with equal mass densities, most of the initial activity would involve mass exchanges between the smaller grains. In the second example, the metamorphisms of fine-grained and large-grained snow were compared. In this case, it was seen that metamorphism was much more dynamic for the fine-grained snow. The calculations also showed that temperature does significantly affect the rate of metamorphism. Finally, the effect of initial grain size distribution on the rate of grain growth was considered. The calculated results demonstrated that initial grain size distribution does not appear to dramatically affect long-term grain growth. In the example used here, the material with an initial uniform size distribution experienced an initial larger grain growth rate. However, its grain size distribution slowly evolved towards one similar to the other material, with the result that its grain growth rate approached that of the second sample. It remains to be seen if this would also be the case under conditions involving large Temperature gradient. Experimental data forthcoming with improved image analysis methods should help determine if this result is representative of what really happens.

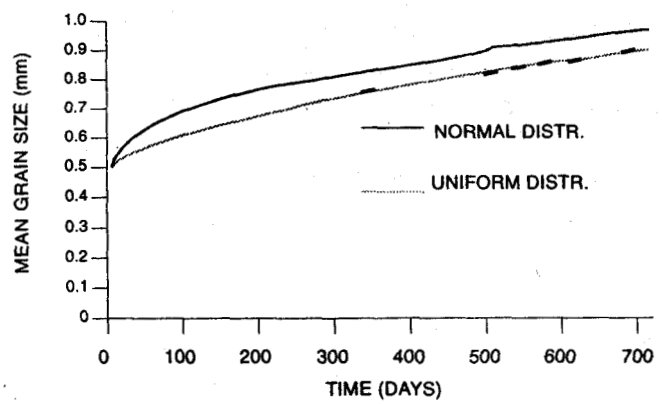

Figure 9. Comparison of the rate of change in mean grain size for two grain size distributions.

Work is continuing to compare these results with those of stereology studies currently underway. In addition, the formulation presented here is

now being applied to equitemperature conditions involving a nonhomogeneous material with an elastic/viscoplastic behaviour and to temperature gradient conditions.

ACKNOWLEDGEMENT

The research reported here has been funded by the Terrestrial Sciences Programme of the Army Research Office under Grants No. DAAH04-94-G-0092 and DAAL03-91-G-0310. The authors wish to express their appreciation to the Army Research Office for this support.

REFERENCES

1. Truesdell, C. Sulle basi della thermomeccanica. *Rend. Lincei,* Ser.8, 1957, **22**, 158-166.
2. Muller, I. A thermodynamic theory of mixtures of fluids. *Arch. Ration. Mech. Anal.,* 1968, **28**, 1-39.
3. Bowen, R. M. Theory of mixtures, *In* Continuum Physics, edited by A. C. Eringen. Academic Press, 1976.
4. Goodman, M. A. & Cowin, S. C. A continuum theory for granular materials. *Arch. Ration. Mech. Anal.*, 1972, **44**, 249-66.
5. Passman, S. L. Mixtures of granular materials. *Int. J. Engg. Sci.,* 1977, **15**, 117-29.
6. Nunziato, J. W. & Walsh, E. K. On ideal multiphase mixtures with chemical reactions. *Arch. Ration. Mech. Anal.,* 1980, **73**, 285-311.
7. Adams, E. E. & Brown, R. L. A constitutive theory for snow as a continuous multiphase mixture. *Int.J. Multiph. Flow,* 1989, **28**, 205-09.
8. Adams, E. E. & Brown, R. L. A mixture theory for evaluating heat and mass transport processes in nonhomogeneous snow. *Contin. Mech. Thermodyn.,* 1990, **2**, 31-63.
9. Morland, L. W.; Kelly, R. J. & Morris, E. M. A mixture theory for phase changing snowpack. *Cold Regions Sci. Technol.,* 1990, **17**, 271-85.
10. Morland, L. W. Flow of viscous fluids through a porous deformable matrix. *Surface Geophysics,* 1992, **13**, 209-68.
11. Hansen, A.C. Re-examining some basic definitions of modern mixture theory. *Int. J. Multiph. Flow,* 1991, **30** (12), 1531-34.
12. Hansen, A.C.; Crane, R.L.; Damson, M.H.; Donovan, R.P.; Horning, D. T. & Walker, J. L. Some notes on a volume fraction mixture theory and a comparison with the kinetic theory of gases. *Int. J. Multiph. Flow,* 1991, **30** (5), 561-73.
13. Reid, C. D. & Jafari, F. The kinematics and general field equations for continuum mixtures. *Int. J. Engg. Sci.,* 1995, **33**(3), 411-28.
14. Gray, J.M.N.T. & Morland, L. W. A dry snow pack model. *Cold Regions Sci. Technol. 1994,* **22**, 35-148.
15. Maeno, N. & Ebinuma, T. Pressure sintering of ice and its implication to densification of snow at polar glaciers and ice sheets. *J. Phys. Chem.,* 1983, **87**(21), 4103-10.
16. Edens, M. Q. & Brown, R. L. On the relation between neck length and bond radius of snow during compression, *Journal of Glaciology,* 1990, **37**(126), 203-08.